

# Hydrolytic Metalloenzyme Models. Effects of AOT Reverse Micelles on the Hydrolysis of *p*-Nitrophenyl Picolinate Catalyzed by $\text{Zn}^{2+}$ and $\text{Cu}^{2+}$ Complexes of *N*-Alkyl-2-hydroxymethylimidazoles

Tsune-hisa FUJITA, Yoichi INABA, Kenji OGINO, and Waichiro TAGAKI\*  
 Department of Applied Chemistry, Faculty of Engineering, Osaka City University,  
 Sugimoto 3, Sumiyoshi-ku, Osaka 558  
 (Received September 26, 1987)

The catalytic effects of bivalent metal ion ( $\text{Zn}^{2+}$  and  $\text{Cu}^{2+}$ ) complexes of *N*-alkyl-2-hydroxymethylimidazoles on the hydrolysis of *p*-nitrophenyl picolinate (PNPP) have been studied kinetically in the reverse micelles of AOT/hexane/water at 25 °C. The results were compared with those obtained in the non-micellar aqueous media and aqueous micelles. The hydrolysis was observed to occur through the acyl group transfer from PNPP to the ligand hydroxyl group in both cases of  $\text{Zn}^{2+}$  and  $\text{Cu}^{2+}$  ions and in all three non-micellar and micellar systems. However, the ligand:metal ion ratio in the kinetically active complexes was found to differ significantly in the three systems: there seems to exist general trends of 1:1, 2:1, and 4:1 stoichiometry in the ligand:metal ion ratio, depending on non-micellar aqueous media, aqueous micelles and reverse micelles, respectively. It was also noticed that the hydrolysis is always faster in micellar systems than in non-micellar aqueous media. Furthermore, a lipophilic ligand (*N*-dodecyl, Lig-12) was found to be more active than a hydrophilic ligand (*N*-methyl, Lig-1) under two micellar conditions.

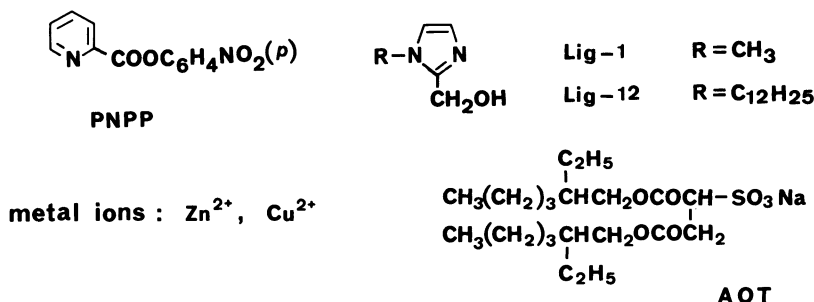
The micellar catalysis has been extensively studied for the past two decades as the model of enzyme catalysis.<sup>1)</sup> However, as for the micellar models of hydrolytic metalloenzymes, the studies appear to begin only recently.<sup>2–7)</sup> In 1980, we reported that *N*-dodecyl-2-hydroxymethylimidazole (Lig-12) is remarkably active for the hydrolysis of *p*-nitrophenyl picolinate (PNPP) when complexed with  $\text{Zn}^{2+}$  ion and co-micelled in surfactant micelles in aqueous media.<sup>2)</sup> Later studies revealed that Lig-12 is even more active in the presence of  $\text{Cu}^{2+}$  ion.<sup>3)</sup>

Besides the aqueous micelles, there are also known reverse micelles in apolar solvents. Namely, certain surfactants such as sodium 1,2-bis(2-ethylhexyloxy-carbonyl)ethanesulfonate (AOT) can solubilize water in apolar organic solvents to form reverse micelles.<sup>1)</sup> In such reverse micelles, the surfactant polar heads entrap water molecules as water pools in the cores, while the surfactant hydrocarbon chains extend toward the outer bulk organic solvent. Such water pools are said to resemble somewhat those entrapped in the active sites of enzymes. Therefore, it may be interesting to see what happen when the above hydrolysis is carried out in reverse micelles. To the best of our knowledge, there has been no such a study

in the literature except those in aqueous micelles<sup>2–7)</sup> as mentioned above. We now wish to report that the bivalent metal ion ( $\text{Zn}^{2+}$  and  $\text{Cu}^{2+}$ ) complexes of *N*-alkyl-2-hydroxymethylimidazoles (Lig-1 and Lig-12) are very active for the hydrolysis of PNPP in the reverse micelles of AOT/hexane/water. The results were also compared with those obtained in the previous studies in aqueous micelles.<sup>2,3)</sup> One might ask why the two metal ions,  $\text{Zn}^{2+}$  and  $\text{Cu}^{2+}$ , are particularly selected for comparison in this work. One reason is that they are widely different in the ability to activate coordinated hydroxyl group as a nucleophile. Another and more interesting reason comes from our recent finding that  $\text{Zn}^{2+}$  ion requires a tetrahedral geometry for the activation of hydroxyl group of bis(imidazole) ligands, while  $\text{Cu}^{2+}$  ion requires square planar geometry for the activation.<sup>8)</sup>

## Results and Discussion

The metal ion salts ( $\text{Zn}(\text{NO}_3)_2$  and  $\text{Cu}(\text{NO}_3)_2$ ) could be solubilized in hexane, only in the presence of both AOT and water. The water component of reverse micelles was the acetate buffer solution (0.1 mol·dm<sup>-3</sup>, pH 4.9). The use of other buffer solutions of higher pH, such as lutidine buffer (pH 7) tended to cause the



precipitation of metal ion hydroxide. Hence only acetate buffer was used in this study. Rates of hydrolysis were determined by measuring released *p*-nitrophenol spectrophotometrically at 310 nm. In all cases, under the conditions containing excess amount of ligand over the substrate (PNPP), good pseudo-first-order rate constants ( $k_{\text{obsd}}$ ) were obtained up to the completion of hydrolysis.

**Effects of AOT and Water.** As shown in Fig. 1, the rates ( $k_{\text{obsd}}$ ) increased initially up to a maximum, then decreased with increasing AOT concentration. Here the concentrations of water and Lig-12 also increased with increasing AOT, while their ratios  $w_o = [\text{water}]/[\text{AOT}]$  and  $[\text{AOT}]/[\text{Lig-12}]$  were kept constant. The curve in Fig. 1 appears to be rather common in the reactions of both aqueous and reverse micelles,<sup>1,9-11</sup> and may be accounted for in the following way. It is generally considered that the size of reverse micelles or

the size of water pools is determined by the  $w_o$  ratio, so that at a constant  $w_o$  as in Fig. 1, the increase in AOT concentration results in the increase in micelle concentration of the same size.<sup>11</sup> Thus the curve of Fig. 1 shows the saturation of rates due to the saturation of incorporation of reactants into micelles ( $\text{Zn}^{2+}$  ion, Lig-12 and PNPP). A slow decrease in rates after the maximum is explained by the dilution of reactants ( $\text{Zn}^{2+}$  and PNPP) per micelle, although the concentration of Lig-12 remains constant.

Next, the effect of  $w_o$  on the rates was examined as shown in Fig. 2. It shows the presence of an optimum value at about  $w_o = 14$ . In the case of AOT, it is considered that the water molecules (in the water pools) up to perhaps  $w_o = 6-8$  are tightly bound to the head groups of the surfactant,<sup>12,13</sup> and above this value the water molecules become free water and the micelles swell when the water content increases.<sup>13,14</sup> Thus the above value  $w_o = 14$  suggests that an appropriate amount of free water is necessary for faster rates. The micellar molecular weight based on the light scattering data will be discussed later.

**Stoichiometry of the Reactive Complexes.** In order to know the stoichiometry of the kinetically reactive complexes, the kinetic version of Job plots<sup>15,16</sup> was examined by plotting the  $k_{\text{obsd}}$  values as a function of mole fraction of ligand ( $\gamma$ ), maintaining the total concentration of ligand and metal ion constant. The results shown in Fig. 3 indicate that in the case of  $\text{Zn}^{2+}$  ion and Lig-12 the rate maximum was observed at  $\gamma = 0.8$  which corresponds to a stoichiometry of ligand: $\text{Zn}^{2+} = 4:1$ . The figure also indicates that the rates are very slow in the presence of metal ion

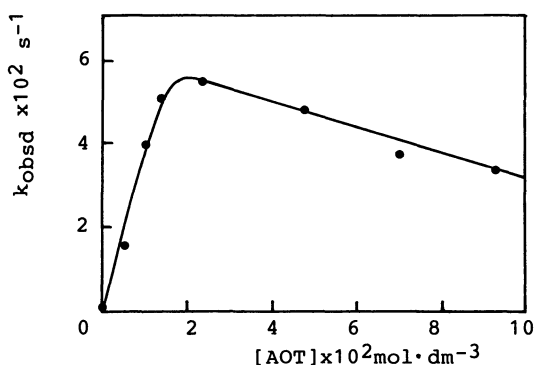


Fig. 1. Pseudo-first-order rate constants for the hydrolysis of PNPP at 25°C as the function of AOT concentration.  $w_o = [\text{H}_2\text{O}]/[\text{AOT}] = 14.1$ ,  $[\text{AOT}]/[\text{Lig-12}] = 22.5$ ,  $[\text{PNPP}] = 5 \times 10^{-5} \text{ mol} \cdot \text{dm}^{-3}$ ,  $[\text{Zn}^{2+}] = 1 \times 10^{-4} \text{ mol} \cdot \text{dm}^{-3}$ .

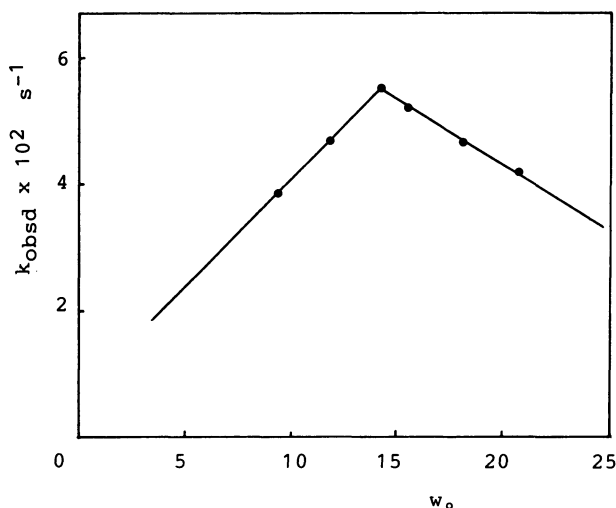


Fig. 2. Pseudo-first-order rate constants for the hydrolysis of PNPP at 25°C as the function of  $w_o$  value.  $[\text{AOT}] = 0.022 \text{ mol} \cdot \text{dm}^{-3}$ ,  $[\text{Zn}^{2+}] = 1 \times 10^{-4} \text{ mol} \cdot \text{dm}^{-3}$ ,  $[\text{PNPP}] = 5 \times 10^{-5} \text{ mol} \cdot \text{dm}^{-3}$ ,  $[\text{AOT}]/[\text{Lig-12}] = 22.5$ .

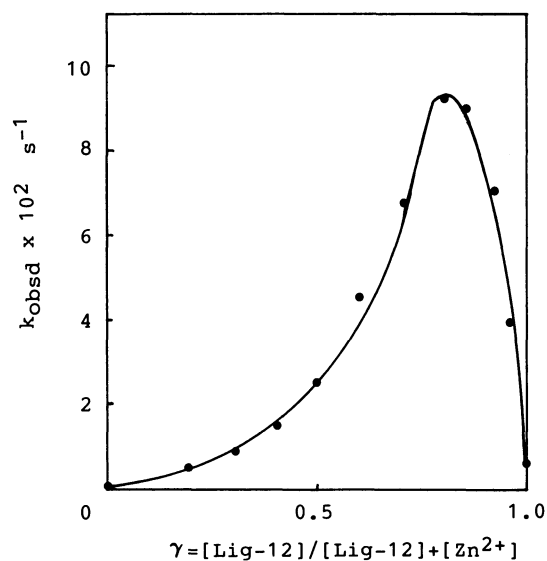


Fig. 3. Job plots for the ligand and  $\text{Zn}^{2+}$  ion complexation as measured by the rates of hydrolysis of PNPP as 25°C.  $[\text{AOT}] = 0.022 \text{ mol} \cdot \text{dm}^{-3}$ ,  $[\text{H}_2\text{O}] = 0.35 \text{ mol} \cdot \text{dm}^{-3}$ ,  $[\text{PNPP}] = 5 \times 10^{-5} \text{ mol} \cdot \text{dm}^{-3}$ ,  $([\text{Lig-12}] + [\text{Zn}^{2+}]) = 1 \times 10^{-3} \text{ mol} \cdot \text{dm}^{-3}$ .

or ligand alone (i.e.  $\gamma=0$  or 1.0). Very similar plots were also obtained in the cases of  $\text{Cu}^{2+}$  ion as shown in Fig. 4, although the absolute values of rates were much larger than those in the case of  $\text{Zn}^{2+}$  ion. Here it should be noticed that lipophilic Lig-12 is more active than hydrophilic Lig-1.

The above 4:1 stoichiometry for Lig-12 is quite different from the 2:1 stoichiometry observed previously for Lig-12 catalysis in aqueous micelles.<sup>2,3</sup> In the case of a hydrophilic Lig-1, the stoichiometry in Fig. 4 is also 4:1. However, this ligand showed a 1:1

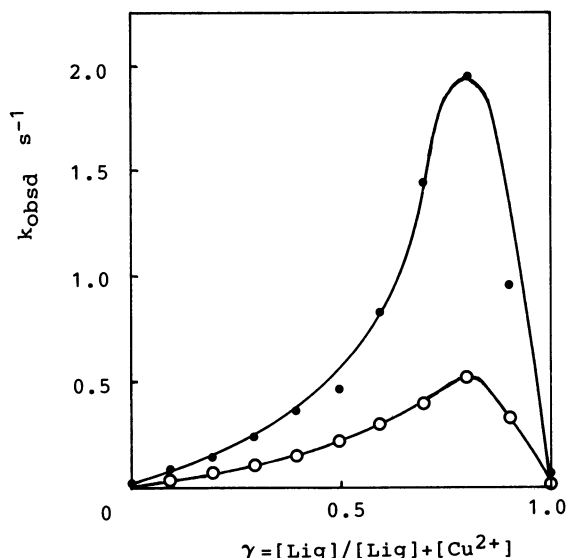


Fig. 4. Job plots for the ligand and  $\text{Cu}^{2+}$  ion complexation as measured by the rates of hydrolysis of PNPP at 25°C.  $[\text{AOT}] = 0.022 \text{ mol} \cdot \text{dm}^{-3}$ ,  $[\text{H}_2\text{O}] = 0.35 \text{ mol} \cdot \text{dm}^{-3}$ ,  $[\text{PNPP}] = 5 \times 10^{-5} \text{ mol} \cdot \text{dm}^{-3}$ ,  $([\text{Lig}] + [\text{Cu}^{2+}]) = 5 \times 10^{-4} \text{ mol} \cdot \text{dm}^{-3}$ , (O): Lig-1, (●): Lig-12.

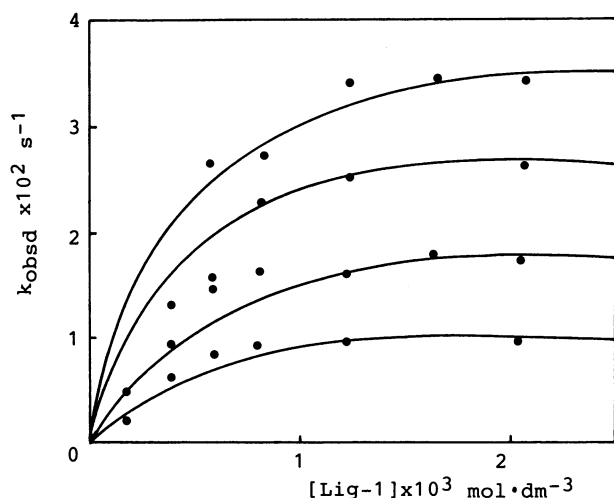


Fig. 5. Pseudo-first-order rate constants for the hydrolysis of PNPP at 25°C as the function of Lig-1 concentration.  $[\text{AOT}] = 0.022 \text{ mol} \cdot \text{dm}^{-3}$ ,  $[\text{H}_2\text{O}] = 0.35 \text{ mol} \cdot \text{dm}^{-3}$ ,  $[\text{PNPP}] = 5 \times 10^{-5} \text{ mol} \cdot \text{dm}^{-3}$ ,  $[\text{Zn}^{2+}] \times 10^4 \text{ mol} \cdot \text{dm}^{-3}$  from the top: 2.0, 1.5, 1.0, and 0.5.

stoichiometry in the previous catalysis in non-micellar aqueous solutions.<sup>3,17</sup> Thus, although it was difficult to see the stoichiometry for lipophilic Lig-12 in non-micellar aqueous media because of a low solubility of the ligand, it appears that there exist general trends of 1:1, 2:1, and 4:1 stoichiometry, depending on non-micellar aqueous media, aqueous micelles, and reverse micelles used, respectively. The reason for these differences in stoichiometry is not clear at present. It seems important to know more details about the hydration of metal ions under these different conditions before making any concrete discussions.

**Second-Order Rate Constant,  $k_c$ .** The  $k_{\text{obsd}}$  values were dependent on the concentrations of both  $\text{Zn}^{2+}$  ion and ligand as shown by four saturation curves in Fig. 5. These curves can be accounted for by assuming the following reaction Scheme 1.



Scheme 1.

In Scheme 1, metal ion (M) and  $n$  ligand (L) form a complex with an association constant ( $K$ ). Then the complex reacts with the substrate (S) to give products with the second-order rate constant ( $k_c$ ). The substrate also goes to the products by other pathways with the rate constant ( $k'_o$ ). The contributing pathways to  $k'_o$  may be the uncatalyzed ( $k_o$ ) and the catalyzed by metal ion ( $k_M[\text{M}]$ ) and ligand ( $k_L[\text{L}]$ ).

The Scheme 1 leads to the rate equations, Eqs. 4—7.

Thus the pseudo-first-order rate constants,  $k_{\text{obsd}}$ , can be represented by Eq. 5. This equation would allow to obtain the  $k_c$  value if the complex concentration could be calculated.

$$\text{Rate} = k_{\text{obsd}}[\text{S}] \quad (4)$$

$$k_{\text{obsd}} = k'_o + k_c [\text{Complex}] \quad (5)$$

$$k'_o = k_o + k_L[\text{L}] + k_M[\text{M}] \quad (6)$$

$$k_{\text{obsd}}^{\text{sat}} = k'_o + k_c[\text{M}]_{\text{T}} \quad (7)$$

However, such was difficult because of the difficulty in determining the association constant,  $K$  in Eq. 1. Therefore, we assumed the Eq. 7 in order to calculate  $k_c$  value on the following ground. Namely, we assumed in Figs. 5 and 6 that the complex concentration at the rate saturation ( $k_{\text{obsd}}^{\text{sat}}$ ) is equal to the total metal ion concentration ( $[\text{M}]_{\text{T}}$ ). In the case of  $\text{Zn}^{2+}$  ion, it was also assumed that the 4:1 ligand:metal ion ( $n=4$ ) complex is formed at the rate saturation. The Eq. 7 requires a straight line relationship in the plots of  $k_{\text{obsd}}^{\text{sat}}$  vs. metal ion concentration. This was

confirmed by the plots shown in Fig. 7. The  $k_c$  values obtained from the slope of these straight lines are shown in Table 1. Figure 7 also indicates  $k'_0$ , the intercepts of the straight lines, to be negligibly small.

In the case of  $\text{Cu}^{2+}$  ion, the plots of  $k_{\text{obsd}}$  vs. ligand concentration are shown in Figs. 8 and 9. The figures indicate that the rates increase steeply to a peak, then decrease sharply with increasing ligand concentration. At first glance, it seems difficult to make reasonable analysis of such complicated curves. More careful look, however, indicates that with increasing  $\text{Cu}^{2+}$  ion concentration (from the lower to the upper),

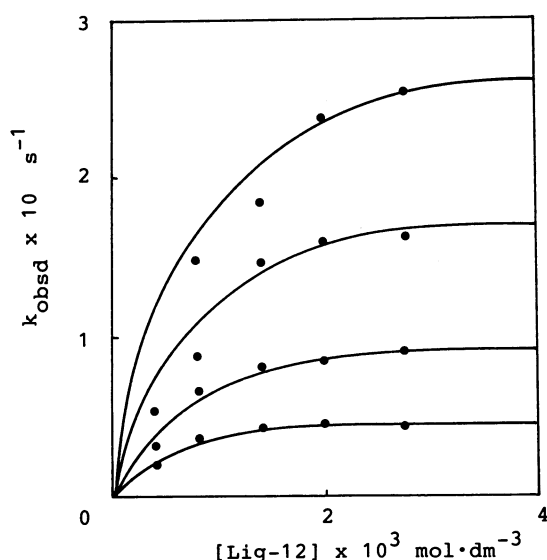


Fig. 6. Pseudo-first-order rate constants for the hydrolysis of PNPP at 25°C as the function of Lig-12 concentration.  $[\text{AOT}] = 0.022 \text{ mol} \cdot \text{dm}^{-3}$ ,  $[\text{H}_2\text{O}] = 0.35 \text{ mol} \cdot \text{dm}^{-3}$ ,  $[\text{PNPP}] = 5 \times 10^{-5} \text{ mol} \cdot \text{dm}^{-3}$ ,  $[\text{Zn}^{2+}] \times 10^4 \text{ mol} \cdot \text{dm}^{-3}$  from the top: 3.0, 2.0, 1.0, and 0.5.

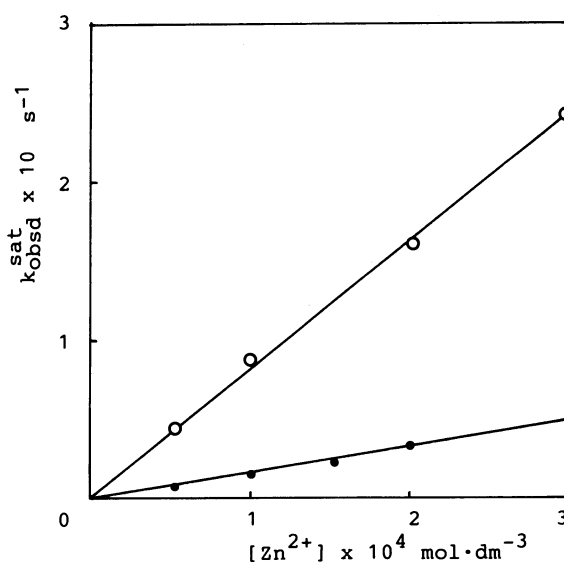


Fig. 7. Plots of  $k_{\text{obsd}}^{\text{sat}}$  in Figs. 5 and 6 as the function of  $\text{Zn}^{2+}$  ion concentration. (●): Lig-1, (○): Lig-12.

the ligand concentration at the peak position approaches to such a value to give  $[\text{ligand}]/[\text{Cu}^{2+}] = 4$ . For example, in Fig. 8 the top curve of  $[\text{Cu}^{2+}] = 2 \times 10^{-4} \text{ mol} \cdot \text{dm}^{-3}$  shows the peak at  $[\text{ligand}] = 8 \times 10^{-4} \text{ mol} \cdot \text{dm}^{-3}$ . This ratio of 4 is the stoichiometry for the reactive complex ( $n=4$  in Scheme 1) determined from Job plots (Fig. 4). Thus the decreasing in rates after the peak in Figs. 8 and 9 suggests the formation of

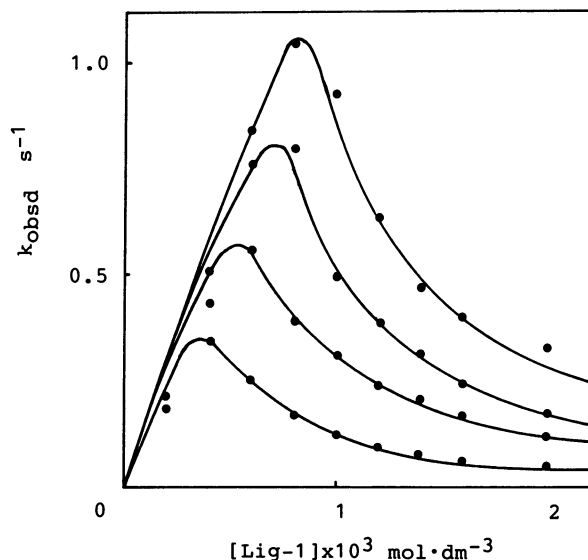


Fig. 8. Pseudo-first-order rate constants for the hydrolysis of PNPP at 25°C as the function of Lig-1 concentration.  $[\text{AOT}] = 0.022 \text{ mol} \cdot \text{dm}^{-3}$ ,  $[\text{H}_2\text{O}] = 0.35 \text{ mol} \cdot \text{dm}^{-3}$ ,  $[\text{PNPP}] = 5 \times 10^{-5} \text{ mol} \cdot \text{dm}^{-3}$ ,  $[\text{Cu}^{2+}] \times 10^4 \text{ mol} \cdot \text{dm}^{-3}$  from the top: 2.0, 1.5, 1.0, and 0.5.

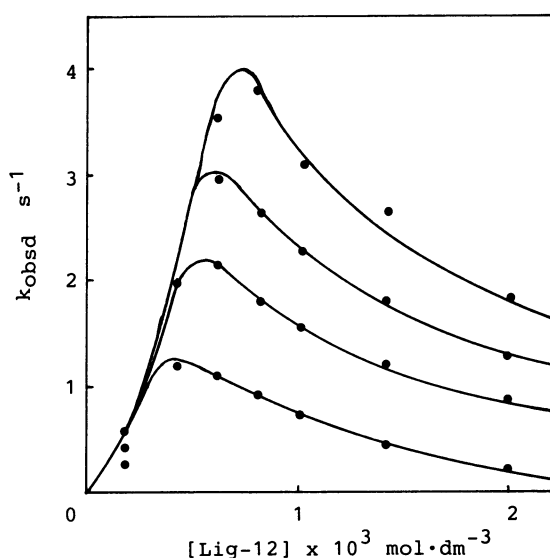


Fig. 9. Pseudo-first-order rate constants for the hydrolysis of PNPP at 25°C as the function of Lig-12 concentration.  $[\text{AOT}] = 0.022 \text{ mol} \cdot \text{dm}^{-3}$ ,  $[\text{H}_2\text{O}] = 0.35 \text{ mol} \cdot \text{dm}^{-3}$ ,  $[\text{PNPP}] = 5 \times 10^{-5} \text{ mol} \cdot \text{dm}^{-3}$ ,  $[\text{Cu}^{2+}] \times 10^4 \text{ mol} \cdot \text{dm}^{-3}$  from the top: 2.0, 1.5, 1.0, and 0.5.

unreactive or less reactive complex(es) chelated with more than four ligands ( $n > 4$ ). It is reasonable to consider such unreactive complexes to be important for  $\text{Cu}^{2+}$  ion, but not for  $\text{Zn}^{2+}$  ion, since it is well-known that the complexation with imidazoles is much stronger for the former than for the latter metal ion. With these limitations in mind, the  $k_{\text{obsd}}$  values at

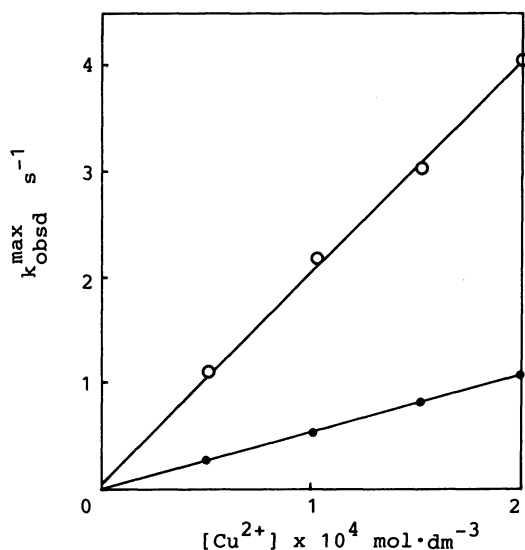


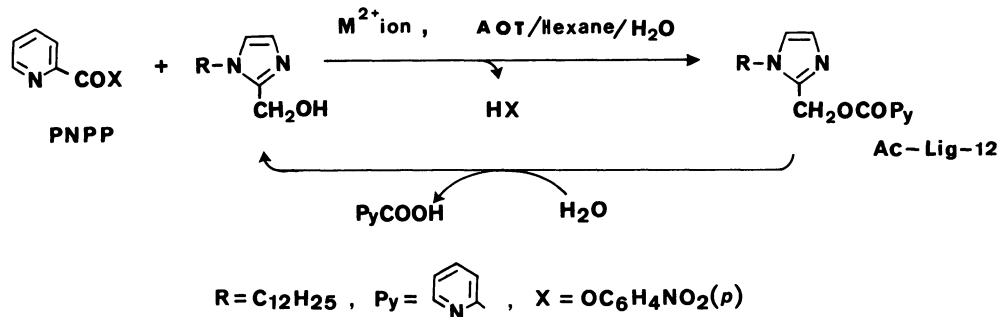
Fig. 10. Plots of  $k_{\text{obsd}}^{\text{max}}$  in Figs. 8 and 9 as the function of  $\text{Cu}^{2+}$  ion concentration. (●): Lig-1, (○): Lig-12.

the peaks ( $k_{\text{obsd}}^{\text{max}}$ ) were plotted as the function of  $\text{Cu}^{2+}$  concentration to give straight lines as shown in Fig. 10. The slopes are the  $k'_c$  values of  $\text{Cu}^{2+}$  complexes which are perhaps slightly smaller than the real  $k_c$  values (see Table 1).

#### General Discussion—Mechanism of Catalysis: a) Two-Step Mechanism Involving Acyl-Intermediate.

The reaction occurs through the acyl group transfer from the substrate (PNPP) to the ligand hydroxyl group in both cases of  $\text{Zn}^{2+}$  and  $\text{Cu}^{2+}$  ions. This was confirmed in two ways for Lig-12 by carrying out the reaction under the conditions of excess substrate over the ligand: (1) kinetically, burst kinetics were observed as described previously,<sup>3</sup> and (2) the acylated intermediate (Ac-Lig-12) was detected by HPLC analysis.<sup>8</sup> Thus the catalytic cycle in the present reverse micelles are essentially the same as reported previously,<sup>3,8</sup> and as illustrated in Scheme 2.

b) The Stoichiometry in the Ligand-Metal Ion Complexation. The results are summarized in Table 1, together with those reported previously for the reactions in non-micellar aqueous media and aqueous micelles.<sup>2,3,17</sup> The table shows no particular difference in the stoichiometry of ligand-metal ion between  $\text{Zn}^{2+}$  and  $\text{Cu}^{2+}$  ions, regardless of the reaction conditions. However, the table clearly indicates that the reaction conditions are important in determining such stoichiometry. It seems likely that the hydration



Scheme 2.

Table 1. Second-Order Rate Constants and the Stoichiometry of the Reactive Complex for the Hydrolysis of PNPP at 25°C

Ligand	Metal ion	pH	Reactive complex Lig:M	$k_c$ or $k'_c$ $\text{mol}^{-1} \text{dm}^3 \text{s}^{-1}$	Ref.
Reverse micelle <sup>a)</sup>					
Lig-1	$\text{Zn}^{2+}$	4.9 <sup>b)</sup>	4 : 1	$1.68 \times 10^2$	This work
	$\text{Cu}^{2+}$	4.9 <sup>b)</sup>	4 : 1	$5.42 \times 10^3$	This work
Lig-12	$\text{Zn}^{2+}$	4.9 <sup>b)</sup>	4 : 1	$0.81 \times 10^3$	This work
	$\text{Cu}^{2+}$	4.9 <sup>b)</sup>	4 : 1	$1.92 \times 10^4$	This work
Normal micelle <sup>c)</sup>					
Lig-12	$\text{Zn}^{2+}$	7.0	2 : 1	$3.70 \times 10^3$	3
	$\text{Cu}^{2+}$	7.0	2 : 1	$3.23 \times 10^5$	3
Non micelle <sup>d)</sup>					
Lig-1	$\text{Zn}^{2+}$	7.0	1 : 1	$1.36 \times 10^2$	3
	$\text{Cu}^{2+}$	7.0	1 : 1	$7.69 \times 10^3$	21

a)  $[\text{AOT}] = 0.022 \text{ mol} \cdot \text{dm}^{-3}$ ,  $[\text{H}_2\text{O}] = 0.35 \text{ mol} \cdot \text{dm}^{-3}$ . b) The pH of added acetate buffer. c)  $[\text{Hexadecyltrimethylammonium bromide}] = 0.01 \text{ mol} \cdot \text{dm}^{-3}$  in aqueous buffer. d) In aqueous buffer.

of metal ions becomes weaker in the order of non-micellar aqueous media  $\gg$  aqueous micelles  $\gg$  reverse micelles, concomitantly with increasing number of ligand coordination. The 1:1 and 2:1 complexes may form the reactive complexes at the transition state by replacing the hydrated water with the substrate as illustrated in Fig. 11 (A and B). The situation seems to be more complicated in the cases of 4:1 complexes in reverse micelles. If they have a tetrahedral structure as generally considered for  $\text{Zn}^{2+}$  complexes, then the ligand exchange with the substrate appears to be necessary before attaining the transition state as illustrated in Fig. 12.<sup>18)</sup>

c) **The Molecular Weight of the Present AOT Reverse Micelle—an Attempt to Visualize the Catalytic Site.** Self aggregation in AOT reverse micelles has been relatively well-investigated,<sup>1)</sup> as compared to that in other surfactants. As mentioned above, it is considered that the size and the aggregation number ( $N$ ) of AOT reverse micelles are determined by the  $w_o$  value. In this study, the weight average molecular weight ( $M_w$ ) of AOT reverse micelles in hexane was determined by light scattering method, under the conditions of  $w_o=13$  and by treating a composite micellar aggregate (AOT plus water) to be a single molecule. The  $M_w$  found is  $8.96 \times 10^4$  which corresponds roughly to the composition of 130 of AOT

molecules ( $N=130$ ) and 1700 molecules of water. Day et al. reported the characterization of water-containing reverse micelles of AOT by viscosity and dynamic light scattering methods.<sup>19)</sup> Their data indicate that there is the same straight line relationship between  $N$  and  $w_o$  in the range of  $w_o=3-8$  for three solvents (cyclohexane, toluene, and chlorobenzene), and the extrapolated value is approximately  $N=170$  at  $w_o=13$  which may be in fair agreement with the present  $N=130$ . The above  $M_w$  value practically unchanged in the presence of metal ions and ligand in the present concentration range.

The above data may be used to visualize the catalytic site of the present reverse micelles as in the following way: the use of  $[\text{AOT}]=0.022 \text{ mol} \cdot \text{dm}^{-3}$  with  $w_o=13$ ,  $[\text{Lig}]=4 \times 10^{-4} \text{ mol} \cdot \text{dm}^{-3}$ ,  $[\text{M}^{2+}]=1 \times 10^{-4} \text{ mol} \cdot \text{dm}^{-3}$ , and  $[\text{PNPP}]=5 \times 10^{-5} \text{ mol} \cdot \text{dm}^{-3}$  results in the formation of  $[\text{micelle}]=0.022/130=1.7 \times 10^{-4} \text{ mol} \cdot \text{dm}^{-3}$  and each micelle contains about one molecule of 4:1 ligand-metal ion complex, and 0–1 molecule of substrate.

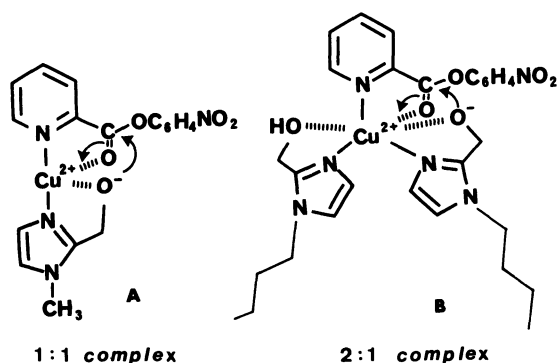


Fig. 11. Schematic illustrations of transition state structures for the non-micellar (A) and for the aqueous micellar (B) systems. (Ref. 2, 3, 17)

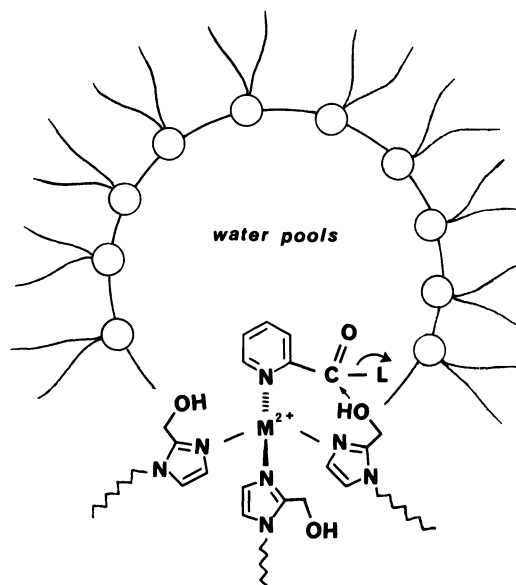


Fig. 13. Oversimplified picture of the catalytic site of AOT reverse micelles composed of bivalent metal ion-ligand complex.

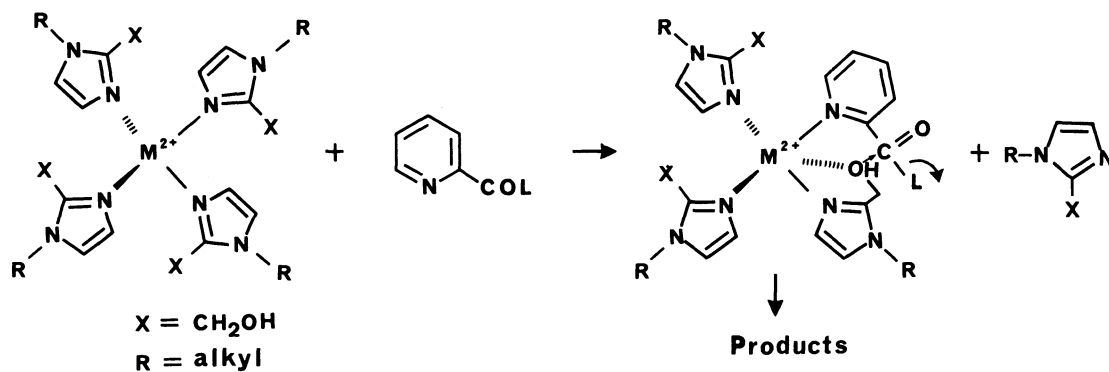


Fig. 12. Very speculative illustration of reaction pathway for 4:1 complexes.

Such a catalytic site at the transition state may be drawn schematically as in Fig. 13.

### Experimental

**Material.** The water used for kinetics was obtained by distilling deionized water. Benzene and hexane were distilled from sodium metal (wire) before use. Acetonitrile was distilled from phosphorus pentoxide. Buffer reagents of acetic acid and sodium acetate were commercial extra pure reagents. Commercially available metal salts,  $\text{Zn}(\text{NO}_3)_2 \cdot 6\text{H}_2\text{O}$  and  $\text{Cu}(\text{NO}_3)_2 \cdot 6\text{H}_2\text{O}$  were used without further purification. Commercially available sodium 1,2-bis(2-ethylhexyloxycarbonyl)ethanesulfonate (AOT, Nakarai Chemicals, Ltd.) was used without further purification. *N*-Methyl(Lig-1) and *N*-dodecyl-2-hydroxymethylimidazole (Lig-12) were prepared according to the previous method:<sup>2,9</sup> Lig-1, mp 118–120 °C; Lig-12, mp 56 °C.

**Water Content Analysis.** The water contents of the AOT solutions in hexane were determined by the Karl Fischer method, using an apparatus of Kyoto Electronics Manufacturing Co., Ltd. (MKA-3).

#### Examination of Micellar Aggregate by Light Scattering.

The weight average molecular weight ( $M_w$ ) of AOT/water aggregate in hexane was determined by light scattering photometry using Union Giken light scattering apparatus (LS-601). The light source (632.8 nm) was an Ne-He laser. The differential refractive increments of the sample solutions were measured in a Union Giken differential refractometer (RM-102). The sample solutions ( $[\text{AOT}] = 0.0022\text{--}0.018 \text{ mol} \cdot \text{dm}^{-3}$ ,  $w_o = 13$ ) were prepared by sealing them in a quartz glass cell after optical purification by repeated filtration through 0.5  $\mu\text{m}$  millipore filter (Nihon Millipore Kogyo). The  $M_w = 8.96 \times 10^4$  (at  $w_o = 13$ ) was obtained by Debye plots using Rayleigh ratio,  $R_{90}$ .<sup>20</sup>

**Kinetic Measurements.**<sup>2,3,8,17</sup> The reaction was initiated by introducing 15  $\mu\text{l}$  of a substrate stock solution in benzene into 3 ml of a reverse micellar solution of AOT in hexane/aqueous buffer containing the metal ions and the ligand of desired concentrations and maintained at 25 °C. The rate of hydrolysis of PNPP was followed by monitoring the increase of absorbance at infinite time determined for each run and by using the integrated first-order equation  $k_{\text{obsd}} = (2.03/t) \log[(\text{OD}_\infty - \text{OD}_t)/(\text{OD}_\infty - \text{OD}_0)]$ .

The authors thank Prof. Takayuki Ohtsu and Mr. Akikazu Matsumoto for their assistance in carrying out the light scattering experiments.

This research was supported in part by a Grant-in-Aid for Scientific Research No. 60470097 from the Ministry of Education, Science and Culture.

### References

- 1) J. H. Fendler, "Membrane Mimetic Chemistry," Wiley, New York (1982).
- 2) T. Eiki, M. Mori, S. Kawada, K. Matsushima, and W. Tagaki, *Chem. Lett.*, **1980**, 1431.
- 3) W. Tagaki and K. Ogino, *Top. Curr. Chem.*, **128**, 145 (1985).
- 4) C. D. Gutsche and G. C. Mei, *J. Am. Chem. Soc.*, **107**, 7965 (1985).
- 5) S. H. Gellman, R. Petter, and R. Breslow, *J. Am. Chem. Soc.*, **108**, 2388 (1986).
- 6) F. M. Menger, L. H. Gan, E. Johnson, and D. H. Durst, *J. Am. Chem. Soc.*, **109**, 2800 (1987).
- 7) R. Fornasier, D. Milana, P. Scrimin, and U. J. Tonellato, *J. Chem. Soc., Perkin Trans. 2*, **1986**, 233.
- 8) K. Ogino, N. Kashihara, T. Fujita, T. Ueda, T. Isaka, and W. Tagaki, *Chem. Lett.*, **1987**, 1303.
- 9) C. A. Bunton, "Reactions in micelles and similar self-organized aggregates," in "The Chemistry of Enzyme Action," ed by M. I. Page, Elsevier, Amsterdam (1984); Chap. 13, pp. 461–504.
- 10) P. L. Luisi, *Angew. Chem., Int. Ed. Engl.*, **24**, 439 (1985).
- 11) K. Martinek, A. V. Levashov, N. Klyyachko, Y. L. Khmelnitski, and V. Berezin, *Eur. J. Biochem.*, **155**, 453 (1986).
- 12) M. Zulauf and H. F. Eicke, *J. Phys. Chem.*, **83**, 480 (1979).
- 13) M. Wong, J. K. Thomas, and T. Nowak, *J. Am. Chem. Soc.*, **99**, 4730 (1977).
- 14) H. F. Eicke and J. Rehak, *Helv. Chem. Acta*, **59**, 2883 (1976).
- 15) A. Martell and S. Chabarek, "Organic Sequestering Agents," Wiley, New York (1959), p. 508.
- 16) D. S. Sigman and C. T. Jorgensen, *J. Am. Chem. Soc.*, **94**, 1724 (1972).
- 17) K. Ogino, K. Shindo, T. Minami, W. Tagaki, and T. Eiki, *Bull. Chem. Soc. Jpn.*, **56**, 1101 (1983).
- 18) In the cases of bis-imidazole ligands in aqueous micelles, the  $\text{Cu}^{2+}$  ion complexes with 4 imidazole units were all inactive (Refs. 3 and 8).
- 19) R. A. Day, B. H. Robinson, J. H. R. Clarke, and J. V. Doherty, *J. Chem. Soc., Faraday Trans. 1*, **75**, 132 (1979).
- 20) P. Debye, *J. Phys. Colloid Chem.*, **51**, 18 (1947).
- 21) K. Ogino, O. Tanaka, K. Machiya, N. Kashihara, and W. Tagaki, *J. Chem. Soc., Perkin Trans. 1*, in contribution.